Chapter 16
A PRC Description of How Inhibitory Feedback Promotes Oscillation Stability

Farzan Nadim, Shunbing Zhao, and Amitabha Bose

Abstract Using methods of geometric dynamical systems modeling, we demonstrate the mechanism through which inhibitory feedback synapses to oscillatory neurons stabilize the oscillation, resulting in a flattened phase-resetting curve. In particular, we use the concept of a synaptic phase-resetting curve to demonstrate that periodic inhibitory feedback to an oscillatory neuron locks at a stable phase where it has no impact on cycle period and yet it acts to counter the effects of extrinsic perturbations. These results are supported by data from the stable bursting oscillations in the crustacean pyloric central pattern generator.

1 Introduction

Oscillations in the nervous system often originate from neurons that have intrinsic pacemaker properties or from populations of neurons that are coupled with excitatory connections or gap junctions that result in synchronous patterned activity (Grillner, Markram, De Schutter, Silberberg, & LeBeau 2005). While purely inhibitory circuits can give rise to oscillations in the absence of excitation (Bartos

F. Nadim (✉)
Department of Mathematical Sciences, New Jersey Institute of Technology, Newark, NJ, USA

Department of Biological Sciences, Rutgers University, Newark, NJ, USA
e-mail: farzan@njit.edu

S. Zhao
Department of Biological Sciences, Rutgers University, Newark, NJ, USA
e-mail: shunbing@gmail.com

A. Bose
Department of Mathematical Sciences, New Jersey Institute of Technology, Newark, NJ, USA

School of Physical Sciences, Jawaharlal Nehru University, New Delhi, India
e-mail: bose@njit.edu

N.W. Schultheiss et al. (eds.), *Phase Response Curves in Neuroscience: Theory, Experiment, and Analysis*, Springer Series in Computational Neuroscience 6,
DOI 10.1007/978-1-4614-0739-3_16,

et al. 2007; Friesen 1994; Manor et al. 1999), feedback inhibition in pacemaker or excitatory oscillatory networks has been proposed to be important in determining the oscillation frequency (Borgers & Kopell 2003; Wang & Buzsaki 1996; Whittington et al. 2000). Alternatively, feedback inhibition may be prevalent but have little effect on network oscillation frequency. In such cases inhibition has been proposed to promote stability in the oscillatory network (Mamiya & Nadim 2004; Thirumalai, Prinz, Johnson, & Marder 2006).

We examine the idea of feedback inhibition as a promoter of oscillation stability, motivated by our recent data in the pyloric central pattern generator (CPG) of crustacean decapods in which the absence of feedback inhibition leads to a larger variability in the relatively stereotyped triphasic oscillations (freq $\sim$1 Hz). We provide experimental evidence that oscillations in this CPG have less variability in response to perturbations and the effect of factors that inherently increase variability, such as intercircuit interactions, is buffered by the inhibitory synapse. Our results include a demonstration that the experimentally measured phase-resetting curve (PRC) of the pyloric pacemaker neurons lies closer to zero in the presence of feedback inhibition, indicating less sensitivity to extrinsic inputs.

We use a generic two-variable neuronal oscillator model to demonstrate how feedback inhibition can act to increase stability. This model has a typical cubic nullcline and is a simplified model built to mimic the activity of the pyloric pacemaker neurons. Our presentation, however, uses the geometric structure and not the details of the model. As such, the argument is quite general and can be expanded to different oscillator types.

2 Model

We use a single cell oscillator(O) described by two equations of the form

$$\begin{aligned} \varepsilon \frac{\mathrm{d}v}{\mathrm{d}t} &= F(v,h) - I_{\mathrm{syn}} - I_{\mathrm{pert}}, \\ \frac{\mathrm{d}h}{\mathrm{d}t} &= G(v,h), \end{aligned} \tag{16.1}$$

where v is the membrane potential, h is a recovery variable, I_{syn} denotes the feedback synaptic current, I_{pert} represents a perturbation of the system and ε is a positive parameter. We denote by P_0 the oscillation period in the absence of synaptic input and perturbations. The synaptic current is given as

$$I_{\mathrm{syn}} = g_{\mathrm{syn}} s(t) \left(v - V_{\mathrm{syn}}\right), \tag{16.2}$$

where V_{syn} is the synaptic reversal potential. $s(t)$ is a periodic function with period P_0 and is equal to 1 for a time duration of D and is equal to 0 at all other times. In our simulations below, we use a two-variable oscillator based on an inactivating calcium current with instantaneous activation and inactivation variable h based on

a simplified model of the pyloric CPG pacemaker AB neuron (Kintos, Nusbaum, & Nadim 2008)[1]. In this model, we have

$$F(v,h) = I_{\text{ext}} - g_{\text{L}}\,(v - E_{\text{L}}) - g_{\text{Ca}} {m_\infty}^3(v) h\,(v - E_{\text{Ca}})\,,$$
$$G(v,h) = (h_\infty(v) - h)/\tau_h(v).$$

We assume that, in the presence of the inhibitory feedback, the oscillator neuron O will oscillate with period P_0 and will lock to a certain phase relationship with the synaptic input (to be explained later). This assumption implies that the inhibitory feedback does not affect the oscillation frequency. The neuron presynaptic to O does not need to be explicitly modeled but will be referred to as F. The feedback synapse arrives periodically and, when active, has a constant conductance. Thus, we can assume that, if O fires at phase 0, then the synaptic feedback has an onset and an offset phase. The onset phase is also referred to as the synaptic phase φ_{syn}. The synaptic duty cycle (s_{DC}) is defined as the ratio between the active duration D of the synapse and the period of O. Thus the offset phase is $\varphi_{\text{syn}} + s_{\text{DC}}$. We will refer to the oscillation of O in the presence of feedback inhibition as the control case and in the absence of inhibition ($g_{\text{syn}} \equiv 0$) as the uninhibited case.

Much of the analysis that we will conduct will be in the v–h phase plane (Fig. 16.1a) where we will track the behavior of the O trajectory in response to both synaptic inputs and perturbations. The $v-$ nullcline is defined as the set of points $\{(v,h)\colon F(v,h) = 0\}$ and the h-nullcline is the set of points $\{(v,h) : G(v,h) = 0\}$. The former is a cubic-shaped curve that has at lower voltage a local maximum $\text{LK}_0 = (v_{\text{LK0}}, h_{\text{LK0}})$ and at higher voltage a local minimum $\text{RK}_0 = (v_{\text{RK0}}, h_{\text{RK0}})$. The left and right branches of the cubic are denoted as LB_0 and RB_0, respectively. The $h-$nullcline is a decreasing sigmoidal shaped curve that, depending on parameters, intersects the $v-$nullcline on the middle or left branch. For the uninhibited case, parameters are chosen such that the intersection of the two nullclines occurs on the middle branch of the v-nullcline, allowing O to exhibit a stable limit cycle (Fig. 16.1a). When the O trajectory is subjected to inhibition from F (for the duration D), $s(t) = 1$. The effect of the synapse is to raise the $v-$nullcline in the v–h phase plane resulting in a new local maximum $\text{LK}_1 = (v_{\text{LK1}}, h_{\text{LK1}})$, local minimum $\text{RK}_1 = (v_{\text{RK1}}, h_{\text{RK1}})$, and left and right branches denoted LB_1 and RB_1(Fig. 16.1b). If the strength of the synapse, which is governed by g_{syn}, is sufficiently large when $s(t) = 1$ the intersection of the $v-$ and $h-$nullcline occurs along LB_1 (Fig. 16.1b, top left black circle). In a neighborhood of this intersection point, the O trajectory will slow its rate of evolution as this point represents a stable fixed point in the $v - -h$ phase space where both $\text{d}v/\text{d}t$ and $\text{d}h/\text{d}t$ equal 0. At other points along LB_1, because of the shape of the h-nullcline—namely that it is

[1] $\varepsilon v' = (i_{\text{ext}} - i_L - i_{\text{Ca}} - i_{\text{syn}})/c_m$; $m_8(v) = 1/(1 + \exp(-(v + 61)/4.2))$; $h_8(v) = 1/(1 + \exp((v + 88)/8.6))$; $\tau_h(v) = (270/(1 + \exp((v + 84)/7.3)))(\exp((v + 162)/30.0)) + 54$; $i_{\text{ext}} = -0.45$, $g_L = 0.3142$, $g_{\text{Ca}} = 1.2567$, $g_{\text{syn}} = 0.0235$(active for 219.4 ms starting at $t_0 = 302$ ms in each cycle), $E_L = -62.5$, $E_{\text{Ca}} = 120$, $E_{\text{syn}} = -80$, $c_m = 7$, $\varepsilon = 1$.

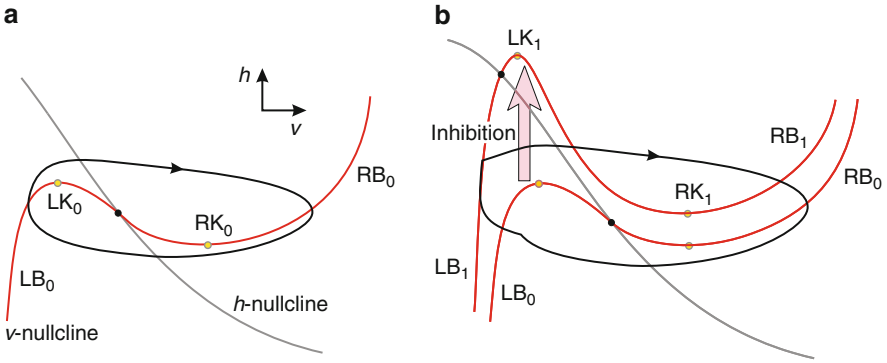

Fig. 16.1 The phase plane of the oscillator neuron.(**a**) In the uninhibited case, the h-nullcline intersects the cubic v-nullcline in the middle branch resulting in an unstable fixed point (filled circle) and a stable limit cycle (*black curve*). (**b**) Inhibition results in a shift of the cubic v-nullcline so that it intersects the h-nullcline in the left branch resulting in a stable fixed point (*filled circle*). Periodic inhibition results in transient movement of the limit cycle trajectory (*black curve*) to the left branch (LB_1) of the inhibited v-nullcline for the duration D of the inhibition. LK/RK denote the local mimima/maxima of the respective v-nullclines. Refer to text for detailed explanation of abbreviations

decreasing and has nonzero slope near LB_0 and LB_1—the rate at which trajectories evolve near LB_1 is greater than near LB_0. The opposite is true for trajectories near RB_1 and RB_0.

For parts of the analysis, we will assume that the system is singularly perturbed (Mishchenko & Rozov 1997). By this, we mean that the parameter ε in (16.1) is small and the O trajectory can by analyzed by separating a slow time scale (t) from a fast one ($\tau = t/\varepsilon$). The fast time-scale governs the rapid increase and decrease of voltage v corresponding to fast depolarization during a spike and repolarization at the end of the spike. The slow time-scale governs the evolution of the slow inactivation variable h during times when the O neuron is in its silent or active state. Mathematically, this separation of time-scales is achieved by setting $\varepsilon = 0$ in (16.1) to obtain the slow subsystem

$$\begin{aligned} 0 &= F(v,h) - I_{\text{syn}} - I_{\text{pert}} \\ \frac{\mathrm{d}h}{\mathrm{d}t} &= G(v,h) \end{aligned} \tag{16.3}$$

or by replacing t with τ in the same equation and then setting $\varepsilon = 0$ to obtain the fast subsystem

$$\begin{aligned} \frac{\mathrm{d}v}{\mathrm{d}\tau} &= F(v,h) - I_{\text{syn}} - I_{\text{pert}}, \\ \frac{\mathrm{d}h}{\mathrm{d}\tau} &= 0. \end{aligned} \tag{16.4}$$

In the singularly perturbed system, the O trajectory lies in a neighborhood of the $v-$nullcline at all moments of time, except when it makes the very fast transitions between the left and right branches of the nullcline. When this reduction is made, the uninhibited O trajectory can be tracked by following the evolution of the slow h-variable along either LB_0 or RB_0 because the evolution of the v-variable can be obtained by solving the constraint $F(v, h) = 0$. The transition between LB_0 and RB_0 occurs from either LK_0 or RK_0 and is assumed to be arbitrarily fast (i.e., taking no time) with respect to the slower h-evolution. This implies that the period of the uninhibited O orbit can be computed by understanding how much time the trajectory spends near LB_0 and RB_0. For the Control case when inhibition is present, whenever $s(t) = 1$, the O trajectory lies close to either LB_1 or RB_1. Thus when $s(t)$ switches from 0 to 1 or vice versa, the trajectory chooses which branch to lie close to. For example, if the trajectory is near LB_0 with $s(t) = 0$, then at the switch to $s(t) = 1$, the trajectory transitions quickly to LB_1. If it were near RB_0 and above the point RK_1 then it transitions to RB_1, but if it were below RK_1, then it would transition to LB_1. Similarly if with $s(t) = 1$ the trajectory is near LB_1 and above LK_0 and $s(t)$ switches to 0, the trajectory jumps to RB_0. Otherwise, it goes to LB_0. Thus, as the onset location and duration of the inhibition changes, the O trajectory will lie in different places in phase space. We will show how this is related to the PRC of the O neuron.

3 Results

3.1 Experimental

We examined the effect of inhibitory feedback on oscillation activity in the crab pyloric network, a pacemaker-driven oscillatory network with an extremely regular oscillation frequency. Pyloric pacemaker (AB and PD) neurons receive their sole inhibitory feedback though a synapse (LP to PD) from the follower neuron LP that bursts out of phase with the pacemakers. Perturbations to the pyloric rhythm arise from many sources, such as the intrinsic noise in pyloric neurons and excitatory inputs from descending projections. We examined whether the LP to PD synapse has an effect on the pyloric cycle period or on how the cycle period is affected by perturbations. After recording the ongoing oscillations (Fig. 16.2; control), the LP to PD synapse was removed by hyperpolarizing the LP neuron (uninhibited). Forty cycle periods were measured in each condition and the cycles immediately following the LP neuron hyperpolarization were not included in this analysis. On average, cycle period was not affected by the removal of the feedback inhibitory synapse; however, the coefficient of variation was significantly smaller in control than uninhibited (Fig. 16.2b). These results suggest that, during the normal ongoing pyloric activity, the LP to PD synapse does not affect the mean network cycle period but it significantly reduces its variability.

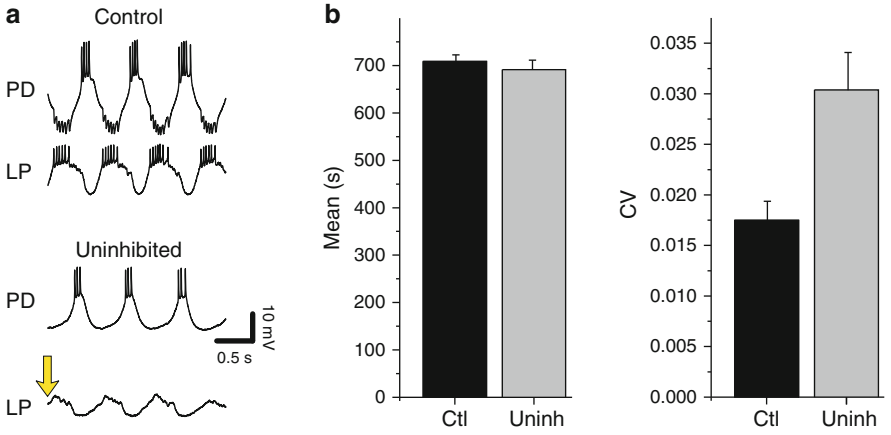

Fig. 16.2 (Experimental) Pyloric oscillation variability is reduced in the presence of the inhibitory feedback synapse but period is not affected. (**a**) Intracellular voltage traces from the pacemaker group neuron PD and the follower LP indicate the activity of pyloric circuit neurons. Recordings were done under control or uninhibited (LP hyperpolarized by injection of -5 nA DC current, arrow, to remove the LP to PD synapse) conditions. (**b**) There was no significant change in the mean pyloric period between control and uninhibited conditions but the coefficient of variation was larger in uninhibited compared to control ($P < 0.05$)

The effect of extrinsic perturbations on the activity of a neural oscillator is often measured by examining the phase-resetting curve (PRC) (Achuthan & Canavier 2009; Oprisan, Thirumalai, & Canavier 2003; Pinsker 1977). To examine the role of the LP to PD feedback inhibitory synapse on the effect of perturbations to the pyloric oscillations, we constructed and compared the PRCs measured by perturbing the PD neuron in control and uninhibited conditions. To construct the PRCs, we injected brief positive current pulses (2 nA, 50 ms) into the PD neuron. Using specialized software (phase response: http://stg.rutgers.edu/software), we injected the current pulses at phases 0.1–0.9 of the cycle to be able to average the response across different trials and preparations. Figure 16.3a shows an example of one such injection under control conditions. Figure 16.3b shows the PRC measured when the reset phase $\Delta\varphi_{\mathrm{PD}} = (P_0 - P)/P_0$ was plotted against the phase of the perturbation $\varphi_{\mathrm{pert}} = \Delta t/P_0$. Here, Δt was measured as the time of the perturbation onset after the first spike in PD burst, P_0 was the free run period, and P was defined as the perturbed period (Fig. 16.3a).

With positive current perturbation the period was prolonged at early perturbation phases and shortened at late phases in both control and uninhibited conditions. However, in the uninhibited case, the perturbations had a stronger effect on the cycle period which was seen in the significant shift of the PRC away from zero compared with the control case. Negative-current perturbations had the opposite effect on cycle period: the period was shortened at early perturbation phases but prolonged at late phases in both conditions (not shown). Yet again, in the control case the PRC was

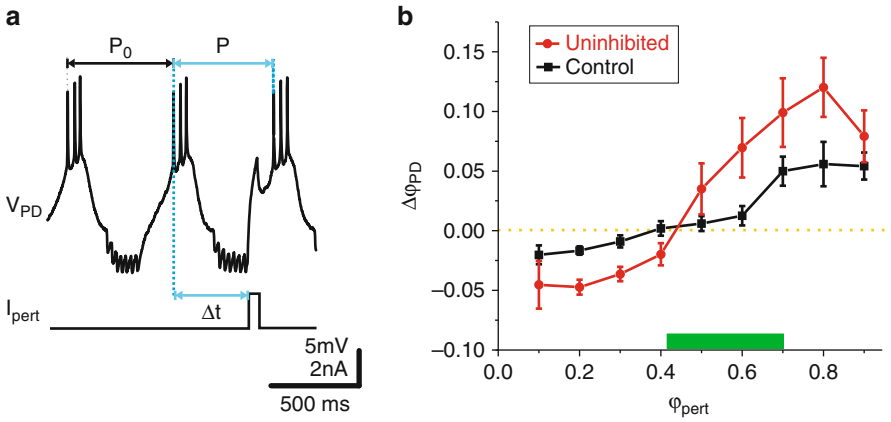

Fig. 16.3 (Experimental) The inhibitory feedback synapse attenuated the effect of extrinsic perturbations as measured through the PRC. (**a**) Intracellular voltage traces from the PD neuron are used to monitor pyloric oscillatory activity. A brief current pulses (2 nA, 50 ms) was injected into the PD neuron at different phases in the presence or absence (not shown) of the LP to PD synapse. (**b**) The PRC in response to the perturbation was measured as the reset phase ($\Delta\varphi_{\mathrm{PD}} = ((P_0 - P)/P_0)$) and plotted against the perturbation phase φ_{pert}. In control, the PRC lies closer to zero compared to uninhibited ($N = 4$). The *green bar* indicates the duration of the synapse activity

closer to zero compared to the uninhibited case. These results show that the LP to PD synapse significantly reduces the effect of perturbations by "flattening" the overall PRC. In particular, there was significant flattening of the PRC even at phases were the synapse was typically not active.

4 Model Description of the PRC Effects

We now turn to our basic mathematical model to explain the observations regarding the PRCs for the two cases. Recall from Fig. 16.2 that the PD neuron cycle period has some natural variability and that this variability is reduced in the presence of the LP to PD feedback inhibitory synapse, as reflected in the cycle period coefficient of variation and more descriptively in the PRC (Fig. 16.3). First, we show that a simplified model as described by (16.1) can reproduce these experimental results. For this, we use the two-variable model of the AB neuron defined in the Model section.

Let $\Lambda(t)$ be a limit cycle of period T of the differential equation $\mathrm{d}X/\mathrm{d}t = f(X)$, $X \in \mathbb{R}^n$. Then the PRC of Λ, for an infinitesimal perturbation vector y can be calculated as the inner product $Z(\varphi) \cdot y$ where $Z(\varphi)$ satisfies the adjoint equation to the linearization of the original differential equation, given by $\mathrm{d}Z/\mathrm{d}t = -A(t)^T Z$, where $A(t) = \mathrm{d}f_{\Lambda(t)}$ (Ermentrout & Terman 2010). The close relationship between

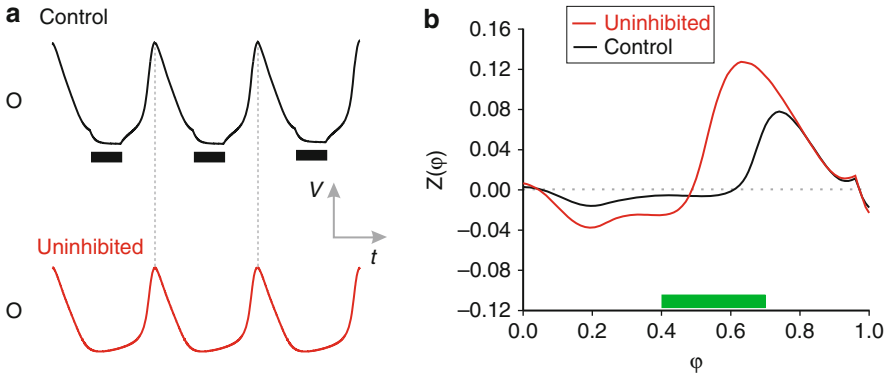

Fig. 16.4 The model PRC lies closer to zero in the presence of feedback inhibition. (**a**) Voltage traces from the model neuron O in the presence (control) and absence(uninhibited) of synaptic inhibition (*black bars*). Both cases have the same cycle period. (**b**) The numerically calculated solutions $Z(\varphi)$ to the adjoint equation calculated at the limit cycle describe the PRC in the control and uninhibited cases. φ represents the phase of the limit cycle. Model as described for the AB neuron in Sect. 2.2.1 and Table 3 of (Kintos et al. 2008). The synaptic input was added from phase 0.3 to 0.7 (*green bar*) of oscillation with $g_{\max} = 0.0235$ nS and $E_{\text{syn}} = -80$ mV

the PRC and the adjoint solution has allowed some researchers to refer to these terms interchangeably. Although adjoint solutions are not always easy to solve for analytically, they can be calculated numerically once a limit cycle has been found (Ermentrout 2002) and graphed to show the shape of the PRC.

Figure 16.4 shows the adjoint solutions $Z(\varphi)$ at the limit cycle, generated for both the control model and when inhibition is removed (uninhibited).The curves $Z(\varphi)$ were generated by numerically calculating the solutions to the adjoint equation of (16.1) at the limit cycle, for one cycle of oscillation, and represent the PRC for an infinitesimal perturbation (Brown et al. 2004). (A similar PRC can be generated by subjecting the trajectories in this model to perturbations of duration 20 ms and amplitude 0.125 nA.) Note that the curves $Z(\varphi)$ shown in Fig. 16.4b qualitatively match the experimental PRCs obtained in Fig. 16.3b.

To explain why the control PRC is generally smaller in amplitude at any phase of the perturbation, i.e., why the oscillation is more robust to perturbation in the presence of the inhibitory feedback synapse, we first introduce the concept of the synaptic phase resetting curve (sPRC). The sPRC documents the change in the O phase as a result of F inhibition and depends primarily on two factors: the synaptic (onset) phase φ_{syn} defined as the phase in the O cycle that the inhibition arrives, and the synaptic duty cycle s_{DC}, defined as the fraction of the cycle that the synapse remains active. To conduct this analysis, we will assume that ε is small and use separation of time scales as described in the Model section above.

Divide the uninhibited O trajectory by phase (φ between 0 and 1 in one cycle), as shown in Fig. 16.5a, such that the point with the maximum voltage along RB_0 is labeled $\varphi_0 = 0$. Label the value φ_1 as the point along RB_0 that has the same h-value

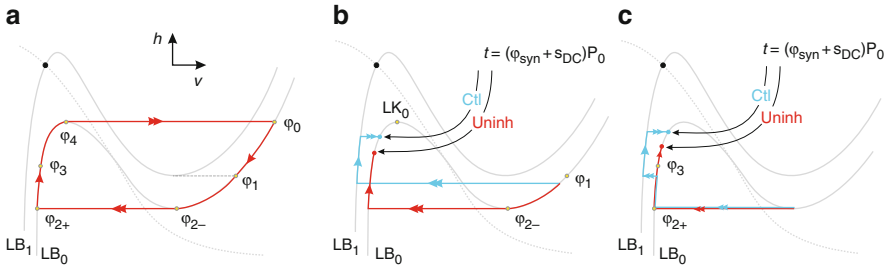

Fig. 16.5 The oscillation phases in the singularly-perturbed case where $\varepsilon = 0$. (**a**) The phase points defined on the uninhibited trajectory. (**b**) Phase relationships for φ_{syn} in $(\varphi_1, \varphi_{2-})$. (**c**) Phase relationships for φ_{syn} in (φ_2, φ_3). Blue trajectory denotes the Control case and the red trajectory is the uninhibited case. The trajectories shown in B and C start at the same time and terminate at the time $t = (\varphi_{\text{syn}} + s_{\text{DC}})P_0$

as RK_1, φ_{2-} as the point RK_0, φ_{2+} as the point on LB_0 with $h = h_{\text{RK0}}$, φ_3 as the point on LB_0 that is $D = s_{\text{DC}} \times P_0$ time away from the point LK_0 but where the evolution is considered using the dynamics along LB_1, and φ_4 as the point LK_0. We will derive the shape of the sPRC using the different phase points defined above. In particular, we will show that the sPRC is a monotone decreasing function of φ_{syn} on a certain interval of phase values. Within this interval, there exists a unique phase φ^* at which the synaptic input from F does not change the O phase. Moreover, we will show that φ^* is a stable attracting phase in the dynamics so that O locks to the synaptic input such that this input always arrives at $\varphi = \varphi^*$. Recall that the synaptic input is periodic with period P_0. This input to O will, in general, change the period of O to a new value we call P. We define $\text{sPRC}(\varphi_{\text{syn}}) = (P_0 - P)/P_0$ and call this the change in phase.

Consider the phase interval $\varphi_{\text{syn}} \in (\varphi_1, \varphi_{2-})$ as shown in Fig. 16.5b. In this case, the effect of the synapse is to shorten P relative to P_0. This happens for two different reasons. First, at the moment the inhibition begins, the trajectory immediately jumps down to LB_1. Thus the phase of the trajectory is advanced because it leaves RB_0 prematurely and does not need to spend time reaching the local minimum point RK_0. Second, for the duration of the inhibition, the trajectory lies on LB_1. Since the speed at which the trajectory evolves (vertically) on LB_1 is greater than on LB_0, the trajectory moves further up in the h-direction on LB_1 than it would have on LB_0. In addition it starts from a higher h-value on LB_1 as shown in Fig. 16.5a. Thus at $t = (\varphi_{\text{syn}} + s_{\text{DC}})P_0$, when the trajectory returns to LB_0, it lies closer to the local maximum point LK_0 than it would have in the absence of the inhibition. Therefore it takes less time to reach LK_0 and as a result $P < P_0$. Therefore $\text{sPRC}(\varphi_{\text{syn}})$ is positive on the interval $(\varphi_1, \varphi_{2-})$.

Next consider the case where φ_{syn} is in the interval $(\varphi_{2+}, \varphi_3)$ as shown in Fig. 16.5c. By the definition of φ_3, for any φ_{syn} in this interval, the trajectory will spend the duration of the inhibition on LB_1 and when the inhibition ends it will return to LB_0 at a point lower than LK_0. Because the evolution rate on LB_1 is larger

than on LB_0 the point to which the trajectory returns to LB_0 will be higher than it would have been in the absence of inhibition. Thus, the remaining time to LK_0 will be less and as above $P < P_0$ which implies that $sPRC(\varphi_{syn}) > 0$. In this interval of synaptic phases, in the singular limit, $sPRC(\varphi_{syn})$ is constant. The reason for this has to do with the fact that there is no time compression between trajectories that receive synaptic inputs during this interval. Let us elaborate by considering two values of φ_{syn} called $\varphi_{synA} < \varphi_{synB}$. The synaptic input corresponding to φ_{synA} arrives when the trajectory is at some h value called h_A. Similarly φ_{synB} arrives at $h = h_B$ with $h_A < h_B$. At this moment in time, there is a certain time distance, say t_d, between the points h_A and h_B that is determined by the rate of evolution along LB_0. After the inhibition starts, both trajectories now evolve along LB_1. There is a new time distance, say t_e, between the h values of the trajectories. But this time remains invariant as long as the trajectories evolve on LB_1. The trajectories spend the same amount of time D on LB_1, before returning to LB_0 where there time distance again becomes t_d. Thus neither trajectory has advanced in phase relative to one another since after the inhibition their time distance apart remains the same as before. This implies that $sPRC(\varphi_{syn})$ is constant on this interval.

The above result is a generic feature of many systems that are decomposed into fast-slow pieces. It follows from the fact that if two trajectories follow the same one-dimensional path for the same amount of time, then, while the Euclidean distance between the trajectories may change, the time distance between them does not. In fact, it is just an application of the group property of flows of a dynamical system (Guckenheimer & Holmes 1997). Finally we note that when we relax, the separation constraint on timescales, $sPRC(\varphi_{syn})$ need not be constant on this interval. Indeed from our numerical simulations, shown later, sPRC may in fact be nonmonotonic. It is not so obvious how to explain why this is the case other than noting that trajectories are no longer constrained to exactly LB_0 and LB_1 and therefore may take slightly different times to reach different locations in phase space. Nonetheless, the fact that $sPRC(\varphi_{syn}) > 0$ for this interval of φ_{syn} follows for the same reasons as above.

If $\varphi_{syn} = \varphi_3$, when the inhibition ends, the trajectory has $h = h_{LK0}$ and immediately jumps back to the RB_0 (Fig. 16.6a). The uninhibited trajectory will lie below $h = h_{LK0}$ still on LB_0 when the control trajectory jumps to RB_0. Now consider the interval (φ_3, φ_4). Since we have already established that $sPRC(\varphi_{syn}) > 0$ at $\varphi_{syn} = \varphi_3$, let us determine what occurs at the opposite end of the interval when $\varphi_{syn} = \varphi_4$ (Fig. 16.6b). Here, the inhibition starts just before the trajectory would have jumped from LK_0 to RB_0. The trajectory, instead, must now spend an amount of time $s_{DC} \times P_0$ on LB_1 until the inhibition ends. Moreover, once the trajectory returns to RB_0, it will have a higher h-value than h_{LK0}. Thus there will be an additional amount of time needed for the trajectory to reach the location of the phase point φ_0. Therefore, $P > P_0$ and $sPRC(\varphi_{syn}) < 0$. By continuity with respect to φ_{syn}, there exists a value $\varphi^* \in (\varphi_3, \varphi_4)$ such that if $\varphi_{syn} = \varphi^*$, then $P = P_0$ and $sPRC(\varphi_{syn}) = 0$. Further, note that the value of φ^* is such that $\varphi^* + s_{DC} \approx 1$.

The synaptic locking phase adjusts itself according to the duration of the synaptic input. To prove uniqueness of φ^*, let us show that $\Delta\varphi$ is monotone decreasing on

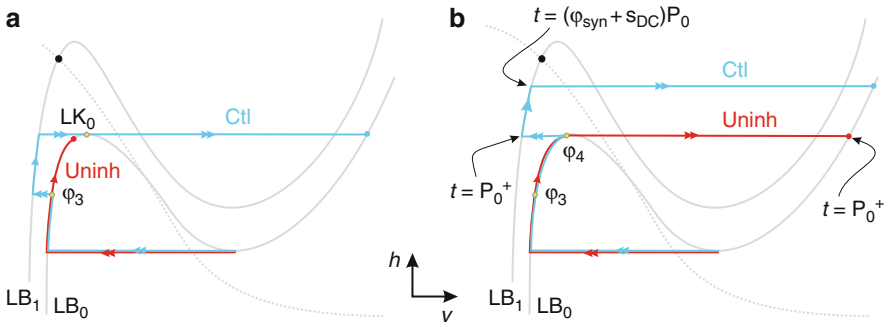

Fig. 16.6 The oscillation phases in the singularly-perturbed case where $\varepsilon = 0$.(**a**) Phase relationships for $\varphi_{\text{syn}} = \varphi_3$. (**b**) Phase relationships for φ_{syn} in (φ_3, φ_4). *Blue* trajectory denotes the control case and the red trajectory is the uninhibited case. The trajectories in both panels start at the same time and terminate at the time $t = (\varphi_{\text{syn}} + s_{\text{DC}})P_0$

this interval. Consider two different values of φ_{syn} denoted φ_{C} and φ_{E}, both in the interval (φ_3, φ_4) such that $\varphi_{\text{C}} < \varphi_{\text{E}}$. When $\varphi_{\text{syn}} = \varphi_{\text{C}}$, the trajectory moves along LB_1 and rises above LK_0 before the inhibition turns off. Say it reaches a point with h-value $h = h_{\text{C}}$. Similarly, when $\varphi_{\text{syn}} = \varphi_{\text{E}}$, the trajectory reaches a point with $h = h_{\text{E}}$ when the inhibition turns off. It is clear that $h_{\text{C}} < h_{\text{E}}$ by continuity with respect to initial conditions since the two trajectories spend the same amount of time on LB_1. Therefore, when the trajectories return to RB_0, the one associated with h_{C} lies below that associated with h_{E}. Now observe that the position of the uninhibited trajectories retain their original orientation. That is the uninhibited trajectory E reaches RB_0 first and begins evolving down, followed at some later time by the uninhibited trajectory C. Define $h(\varphi_{\text{syn}}) = h_{\text{RK}_0} e^{(1-\varphi_{\text{syn}}-s_{\text{DC}})P_0}$ as the value of h along the uninhibited trajectory at the moment its *inhibited* counterpart returns to RB_0. Then, $h(\varphi_{\text{C}}) > h(\varphi_{\text{E}})$ and the following ordering of points holds $h_{\text{E}} > h_{\text{C}} > h(\varphi_{\text{C}}) > h(\varphi_{\text{E}})$. Thus, the change in phase is more for trajectory E than for trajectory C, again implying monotonicity of sPRC on this interval. Therefore, sPRC is monotone decreasing on the interval (φ_3, φ_4) and the value φ^* is unique. To summarize, we have now shown that on the larger interval (φ_1, φ_4), sPRC contains a unique value $\varphi_{\text{syn}} = \varphi^*$ at which the $\text{sPRC}(\varphi_{\text{syn}}) = 0$.

Let us now establish that in the O–F control network, the locked phase φ^* at which $P = P_0$ is a stable, attracting phase of the dynamics (implying that F phase-locks to O activity at phase φ^*).To this end, we define a map f (modulo 1) which records the onset phase φ_{syn} of the synapse at each cycle of inhibition. This map is defined on the interval $[\varphi_1,\varphi_4]$ as the sum of the current synaptic phase and the sPRC at that phase.

$$\varphi_{\text{syn}}^{n+1} = f\left(\varphi_{\text{syn}}^{n}\right)$$
$$f(\varphi) = \varphi + sPRC(\varphi) (\text{mod } 1)$$

In other words, it takes the value of φ_{syn} at one cycle and computes what this value will be at the next cycle. The range of this map is the entire interval [0,1]. This new value of φ_{syn} obviously depends on how the synapse affected the period in the previous cycle and how this changed the phase relationship between O and the F inhibition. From the above analysis, it is easy to establish that $f(\varphi)$ is a continuous function on [0,1], that it has a unique fixed point φ^* and is such that $f(\varphi_1) > \varphi_1$ while $f(\varphi_4) < \varphi_4$.

Proving the stability of φ^* is an exercise in applying the concepts of Fast Threshold Modulation due to Somers & Kopell (1993). Namely, consider two synaptic phases $\varphi_{\text{syn1}} < \varphi_{\text{syn2}}$ in a neighborhood of φ^*. These phases correspond to different h-values $h_i(0)$ at which the trajectory receives the inhibition. There exists a time difference Δt_0 between these two initial conditions which is computed by flowing the trajectory at $h_1(0)$ forward along LB_0 for the time Δt_0 until it reaches the position of $h_2(0)$. When inhibition arrives to these two trajectories, they both move to LB_1 and there exists a new time Δt_1 between them. Since evolution is faster on LB_1 than LB_0, $\Delta t_1 < \Delta t_0$.Both trajectories now flow along LB_1 for exactly the same amount of time $D = s_{\text{DC}} \times P_0$ and the time distance between them remains invariant. After time D, the trajectories are released from inhibition and transition to RB_0, yielding, once there, a new time distance Δt_2. In (Somers & Kopell 1993) conditions are given so that $\Delta t_2 < \Delta t_1$. The main conditions involve a compression factor which is directly related to the rate of evolution on LB_1 immediately before the jump to the rate on RB_0 immediately after the jump. In our case, these rates are strongly governed by the vertical distance of the trajectory to the h-nullcline at these two moments and the time constants governing evolution on those branches. Provided that these time constants are of the same order—a reasonable assumption for bursting neurons—it follows that $\Delta t_2 < \Delta t_1 < \Delta t_0$. This compression in time implies compression in phase. Thus, locally, any two values of φ_{syn} lying in a neighborhood of φ^* are brought closer together by the map f after one iterate. This implies stability of the point φ^*. It must be noted that when φ_{syn1} and φ_{syn2} lie in (φ_2, φ_3), the respective trajectories also make jumps between LB_0, LB_1, and RB_0, as discussed earlier. However, the difference in these phases is that the trajectories return to LB_0 before jumping to RB_0 through the point RK_0. The fact that when φ_{syn1} and φ_{syn2} lie in (φ_3, φ_4) that the trajectories jump from LB_1 directly to RB_0 accounts for the compression.

The stability of φ^* has an immediate consequence. It means that any perturbation applied to the control trajectory will immediately begin to decay due to the fact that $\varphi = \varphi^*$ is the attracting phase and that any change in phase induced by the perturbation will not persist. Later, we will use this observation to show why the PRC for the control case lies closer to 0 than the PRC for the uninhibited case.

Next let us see how the sPRC is affected by the synaptic duty cycle s_{DC}. In Fig. 16.7, we plot numerically-generated examples of the sPRC for three different values of s_{DC}. In general, when s_{DC} decreases, part of the sPRC shifts up in the φ_{syn}–sPRC plane while another portion of it shifts down. Consider two distinct synaptic duty cycles $s_{\text{DC2}} < s_{\text{DC1}}$. To understand which part of sPRC shifts up, first let $\varphi_{\text{syn}} < \varphi_3$, where φ_3 is defined as above but now applied to the s_{DC1} case. The trajectories

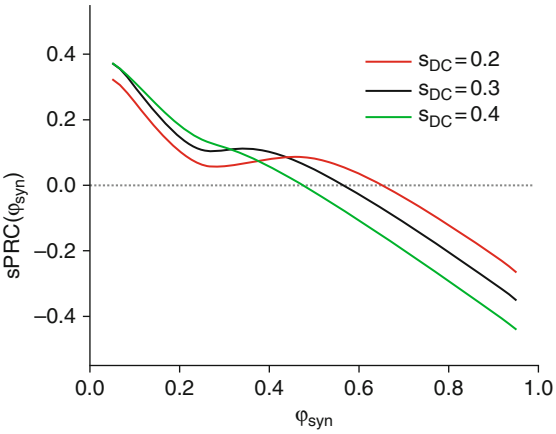

Fig. 16.7 Numerically generated sPRC for different values of s_{DC}. The sPRC was generated for three different values of s_{DC}, 0.2, 0.3 and 0.4, using the model described in Fig. 16.4 with $\varepsilon = 0.14$ to approximate the singular limit. The value φ^* is indicated by the intersection of the sPRC with 0

for both of the s_{DC}'s jump to LB_1 at φ_{syn} and return to LB_0 after the time interval $s_{DCj} \times P_0(j = 1, 2)$ before leaving the silent state through LK_0. Since $s_{DC2} < s_{DC1}$, the trajectory associated with s_{DC2} spends less time on LB_1 than the other trajectory. Therefore, it advances less in phase since the speed of evolution on LB_1 is greater than on LB_0. Thus, the trajectory with longer duty cycle has a greater phase advance for small values of φ_{syn} resulting in the sPRC shifting up as shown in Fig. 16.7 (green curve above black and red). Alternatively, now consider the case where φ_{syn} is larger, say closer to φ_4. Trajectories in both cases will now move along LB_1 to points above LK_0 when the inhibition turns off. The one associated with s_{DC2} will have a smaller $h-$value and will thus need to spend less time on RB_0 to return to the $\varphi = 0$ location. While both trajectories will be delayed in phase relative to the uninhibited trajectory, the s_{DC2} trajectory will be ahead of its counterpart in phase. As a result, the SPRC curve for s_{DC2} will lie above that for s_{DC1} for larger values of φ_{syn} as shown in Fig. 16.7 (red curve above black and green). Note that larger φ_{syn} values have a larger effect on the s_{DC} than smaller φ_{syn} values. At larger φ_{syn}, there are two sources of phase delay. One is the fact that trajectory may still be on LB_1 under the influence of inhibition at the time that the uninhibited trajectory would have returned to RB_0. This means that the trajectory spends extra time on the LB. This occurs for all $\varphi_{syn} \in (\varphi_3, \varphi_4)$. Second, when this happens, the trajectory must also spend extra time on RB_0 while returning to the $\varphi = 0$ starting point. In contrast, changes in s_{DC} have less of an effect for lower values of φ_{syn} as here the different duty cycles simply change the time spent on LB_1, but do not change the fact that these trajectories still leave LB_0 through LK_0 to return to the right branch and the $\varphi = 0$ starting point.

To understand how the sPRC counteracts the effect of perturbations, we first check to see whether the perturbation arrives before, during, or after the inhibition from F. The phase of the perturbation, φ_{pert} is defined with respect to the $\varphi = 0$ reference point on the uninhibited or control trajectory. If $\varphi_{pert} < \varphi^*$, then the uninhibited and control trajectory are roughly following identical paths from $\varphi = 0$

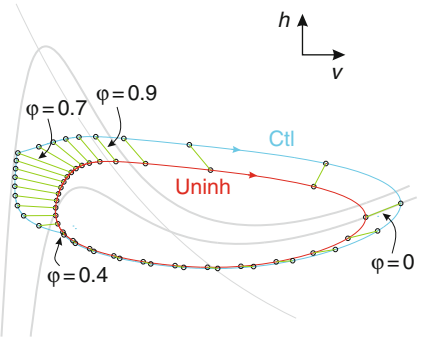

Fig. 16.8 Corresponding phases of the control and uninhibited trajectories. Line segments connect the corresponding phases in the two limit cycles of the model described in Fig. 16.4

to φ_{pert}. For this interval of phases, the sPRC can be composed with the PRC to derive the overall change $\Delta\varphi$ in the phase of O. Specifically, consider an inhibitory perturbation to the control trajectory. This perturbation will change the phase of O by an amount denoted $\Delta\varphi_{\text{prc}}$ and result in a new period P for that cycle. In turn, this causes a change in the value of φ_{syn}. This new value of $\varphi_{\text{syn}} = {\varphi^*}_{\text{syn}} P_0/P$. Since $P = P_0(1-\Delta\varphi_{\text{prc}})$, it follows that $\varphi_{\text{syn}} = {\varphi^*}_{\text{syn}}/(1-\Delta\varphi_{\text{prc}})$. For example, if $\Delta\varphi_{\text{prc}} > 0$, then $\varphi_{\text{syn}} > {\varphi^*}_{\text{syn}}$, which, referring to Fig. 16.7, shows that the O phase is delayed. Further, s_{DC} also changes to a new value given by $s_{\text{DC}} = {s_{\text{DC}}}^*/(1-\Delta\varphi_{\text{prc}})$, where ${s_{\text{DC}}}^*$ refers to the synaptic duty cycle of the unperturbed control case. Denote the effect of sPRC on the O phase by $\text{sPRC}(\varphi_{\text{syn}}, s_{\text{DC}})$. The effects of both the perturbation and sPRC on the change in O phase can be calculated as $\Delta\varphi = \text{sPRC}({\varphi^*}_{\text{syn}}/(1-\Delta\varphi_{\text{prc}}), {s_{\text{DC}}}^*/(1-\Delta\varphi_{\text{prc}}))$. In general, if the perturbation increases O phase, then the sPRC will decrease the O phase and vice versa. This is to be contrasted with the uninhibited trajectory. In that case, any change in phase induced by the perturbation is never counteracted and persists indefinitely.

Let us explore how the sPRC counteracts the perturbation a bit more closely by considering the singular case in which we again impose timescale separation. From before, we know that φ^* satisfies $\varphi^* + s_{\text{DC}} \approx 1$. That is, φ^* adjusts itself so that the time the inhibition turns off corresponds to the time that the control trajectory jumps to RB_0. Thus the above argument about φ_{pert} arriving before the inhibition holds for all $\varphi_{\text{pert}} < \varphi^* = 1 - s_{\text{DC}}$. If $\varphi_{\text{pert}} \in (\varphi^*, 1)$, then the perturbation will change the current value of the O phase, denoted φ_{O}, to some new value, ${\varphi_{\text{O}}}^{\text{new}}$. Note that ${\varphi_{\text{O}}}^{\text{new}}$ is not determined by the PRC of the uninhibited trajectory since the control trajectory does not lie near the uninhibited one for these phases. The perturbed trajectory will lie in a neighborhood of LB_1 until the moment in time that the inhibition ends, which occurs at $t \approx P_0$. Provided that ${\varphi_{\text{O}}}^{\text{new}} > \varphi_3$, the perturbed trajectory will lie above LK_0 at this moment, independent of the actual value of its phase, and at this time, will jump up to LB_0, and spend a small amount of time reaching the $\varphi = 0$ starting point. This argument suggests that, in the singular limit, $\Delta\varphi \approx 0$ for all $\varphi_{\text{pert}} \in (\varphi^*, 1)$.

Next, let us see how the argument extends to the nonsingular case. Now the trajectory spends a nonzero amount of time making the transition from the silent

to the active state. In Fig. 16.8, we show the control and uninhibited trajectories where we have broken up each trajectory by phase and drawn short line segments to indicate places of equal phase along both. Note for this set of parameters, $\varphi^* = 0.4$ and $s_{DC} = 0.3$. The control trajectory stays in a neighborhood of LB_1 from $\varphi = 0.4$ to $\varphi = 0.7$, while from $\varphi = 0.7$ to $\varphi = 1$ it returns to the active state. Note the position of the control and uninhibited trajectories at both $\varphi = 0.4$ and $\varphi = 1$. The control trajectory is longer (in Euclidean distance), but both traverse this range of phases in the same total amount of time. This means that the average speed with which the control trajectory moves in this range of phases is larger than for the uninhibited one. This is most clearly seen for phases in the range (0.4, 0.7) and (0.9, 1) when the control trajectory "catches and passes" the uninhibited trajectory (first in the vertical direction, then in the horizontal direction) in phase space. This observation is not unique to this particular model or parameters we have chosen. Indeed any time two periodic orbits have the same time length, but different total arc lengths over one period, there must be regions in phase space over which the trajectories evolve at different speeds. In our particular case, the main factors governing the speed near LB_0 and LB_1 are the h-dynamics since near these branches dv/dt is close to 0. Across the jump to the active state, the primary factor controlling speed is the vertical distance to the v-nullcline. This can be seen from the fact that both trajectories are relatively flat in the region $(\varphi^*, 1)$ since dv/dt dominates dh/dt across this jump.

Now consider an inhibitory perturbation with phase φ_{pert} between φ^* and $\varphi^* + s_{DC}$. Assume that the perturbation affects them in the same way by shifting them to the left by some amount Δv. For both trajectories, this causes a change in the phase. For the uninhibited trajectory, this change in phase persists for the remainder of the cycle resulting in a new value for the phase as documented by the uninhibited PRC. The situation for the control trajectory is different. Independent of the current phase of the perturbed control trajectory, the synaptic inhibition remains on until at $t = (\varphi^* + s_{DC})P_0$. Note that the trajectory is constrained by the synaptic inhibition to lie close to the inhibited v-nullcline during this time. In particular, at $t = (\varphi^* + s_{DC})P_0$. The perturbed control trajectory will lie in a neighborhood of the $\varphi = \varphi^* + s_{DC}$ point of the control trajectory. This is in fact the key point. Namely, the inhibition places a time constraint on when the perturbed control trajectory can leave LB_1. Thus, because of this constraining effect any phase change the perturbation may have supplied is largely wiped out by the inhibition. For example, if the perturbation had advanced O's phase, the inhibition constrains the trajectory until $t = (\varphi^* + s_{DC})P_0$, counteracting the advance by delaying the trajectory from leaving for the active state until that time. For $t > (\varphi^* + s_{DC})P_0$, the perturbed trajectory lies in a neighborhood of the control trajectory in the v–h phase plane. Thus, any change in phase between the control and perturbed control trajectory is due solely to the minor difference in speed across this jump. In summary for this subcase, the synaptic inhibition largely wipes out any phase resetting supplied by the perturbation. In contrast, in the absence of F inhibition, the phase resetting persists for the entire cycle. The above argument suggests that, as in the singular case, the control PRC should be fairly insensitive to perturbations arriving in the interval

$(\varphi^*, \varphi^* + s_{DC})$ and should thus be quite flat since the only increase in phase is due to slightly different speeds across the jump up to the active state. This is consistent with the PRCs that we computed as shown in Fig. 16.4.

The biggest changes in the PRC occur when φ_{pert} lies between $\varphi^* + s_{DC}$ and 1. Consider an inhibitory perturbation coming during this interval that causes a change $\Delta v < 0$ in both the inhibited and uninhibited trajectories. Now the only difference that the inhibited trajectory has with its uninhibited counterpart is that it lies higher in phase space and thus has a larger dv/dt value over this portion of its orbit. Thus, it can get to the active state more quickly and therefore result in a smaller overall change in phase than the uninhibited trajectory does. Here, there is no direct constraining effect of the synapse. Instead, it is the inhibition that places the control trajectory in a particular part of phase space where it can utilize its advantage in speed to minimize phase changes.

5 Discussion

An important property of many CPG networks is that they exhibit very robust rhythmic oscillations. In many cases, this property is critically important for the proper function of the organism. For example, CPG networks have been shown to control heartbeat, feeding, ventilation, and locomotion (Dickinson 2006; Marder & Calabrese 1996). In all of these cases, stable periodic solutions are necessary for the survival of the animal.

Oscillations often arise in a CPG either through a reciprocally inhibitory pair of neurons or as a result of an endogenous bursting pacemaker neuron(s). In the former case, oscillations are driven by the antiphase interactions of the two neurons. The stability of the oscillations created by this oscillatory pair naturally makes the CPG relatively insensitive to perturbations. In the latter case, however, where oscillations are due to a pacemaker, there is no apparent mechanism that would promote robustness of the rhythm. In this paper, we proposed that a feedback inhibitory synapse that, in general, has no role in creating oscillations instead plays the role of minimizing the pacemaker's sensitivity to perturbations. To demonstrate this capability of the inhibitory neuron, we computed the pacemaker's PRC in the presence and absence of inhibitory feedback. The PRC of a neuron documents the amount that the neuron changes in phase (or period) in response to perturbations applied at different parts of the rhythmic cycle. We showed that the control PRC lies closer to 0 than the uninhibited PRC. This implies that the control pacemaker is less sensitive to perturbations than its uninhibited counterpart.

From a mathematical viewpoint, the effect of the feedback inhibition in making the oscillator less sensitive to perturbations can be explained simply through the notions of neutral and asymptotic stability. The uninhibited oscillator in this model is a neutrally stable limit cycle. While it attracts all trajectories that lie in a neighborhood of itself, it does not assign a phase preference to the attraction. In other words, the perturbed uninhibited trajectory has no means to compensate

the change in phase. This can easily be seen by considering a perturbation of the uninhibited trajectory that lands the perturbed trajectory exactly on the limit cycle itself. Here, the phase is immediately changed, and since the perturbed trajectory is itself on the limit cycle, there will be no additional change in phase. In contrast, the control trajectory is an asymptotically stable limit cycle both in the sense of attracting nearby trajectories and also in the sense of assigning a phase preference. This can be seen through the stability of the fixed point φ^* of the map $f(\varphi_{\text{syn}}) = \varphi_{\text{syn}} + \text{sPRC}(\varphi_{\text{syn}})$. The fixed point φ^* forces the oscillator to lock at a specific phase of the inhibitory feedback. Thus, any perturbation to the control trajectory immediately begins to decay back to the $\varphi = \varphi^*$ fixed point. The rate of decay is governed by the magnitude of the derivative (eigenvalue) obtained through the linearization of the map. The key point is that this decay begins immediately from the moment of the perturbation. This is the reason why the feedback inhibition can have an effect on the period even when the perturbation occurs after the inhibition in that particular cycle has already ended (e.g. for $\varphi_{\text{pert}} > \varphi_{\text{syn}} + s_{\text{DC}}$ in the non-singular cases shown in Fig. 16.4b).

Several other studies have documented how neurons are affected by various synaptic or perturbing inputs. Prinz et al. (2003) found that the PRC of a neuron was more sensitive to the duration of synaptic input than to the strength of the input. This was established by showing that the PRC saturates at biologically plausible synaptic conductances, but continues to change over all biologically realizable synaptic durations (at least in the case of PD neurons). Oprisan et al. (2003) found similar sensitivity to and importance of the duration of short perturbative or longer synaptic inputs in their modeling study in which they reconstructed the PRC of a bursting neuron from time series data. Our work builds on the results of these earlier studies and asks not just how the duration or phase of an input can affect the PRC, but also how two different inputs interact with one another to determine the PRC. In particular, we explored how the perturbation to a pacemaker neuron is buffered by the existence of a specific synaptic component of the network, a component that seemingly has very little effect on the existence or frequency of oscillations in the pacemaker.

Results from our laboratory (Figs. 16.2 and 16.3) and previous experimental studies of the stomatogastric pyloric network show that the inhibitory feedback LP to PD synapse to the pyloric pacemaker neurons has no effect on the average pyloric cycle period in control conditions (Mamiya & Nadim 2004; Zhou, LoMauro, & Nadim, (2006)) even if the synapse is drastically strengthened in the presence of neuromodulators (Thirumalai et al. 2006). We and others had previously proposed that such feedback inhibition may in fact act to stabilize the pyloric rhythm cycle period in response to perturbing inputs (Mamiya & Nadim 2004; Thirumalai et al. 2006). Our current work now demonstrates that the stabilizing effect of feedback inhibition is in fact quite generic and applies to counteract both longlasting perturbations(such as through neuromodulation) that tend to alter network frequency and fast perturbations typically modeled as noise.

Acknowledgments We thank Dr. Lian Zhou for earlier ideas on this work. Supported by NIH MH-60605 (FN), NSF DMS0615168 (AB) and a Fulbright–Nehru Fellowship (AB).

References

Achuthan, S., & Canavier, C. C. (2009). Phase-resetting curves determine synchronization, phase locking, and clustering in networks of neural oscillators. *J Neurosci, 29*(16), 5218–5233. doi: 29/16/5218 [pii] 10.1523/JNEUROSCI.0426–09.2009

Bartos, M., Vida, I., & Jonas, P.(2007). Synaptic mechanisms of synchronized gamma oscillations in inhibitory interneuron networks. *Nat Rev Neurosci, 8*(1), 45–56. doi: nrn2044 [pii] 10.1038/nrn2044

Borgers, C., & Kopell, N.(2003). Synchronization in networks of excitatory and inhibitory neurons with sparse, random connectivity. *Neural Comput, 15*(3), 509–538. doi: 10.1162/089976603321192059

Brown, E., Moehlis, J., Holmes, P., Clayton, E., Rajkowski, J., & Aston-Jones, G.(2004). The influence of spike rate and stimulus duration on noradrenergic neurons. *J Comput Neurosci, 17*(1), 13–29. doi: 10.1023/B:JCNS.0000023867.25863.a4 5273291 [pii]

Dickinson, P. S.(2006). Neuromodulation of central pattern generators in invertebrates and vertebrates. *Curr Opin Neurobiol, 16*(6), 604–614. doi: S0959–4388(06)00148–6 [pii] 10.1016/j.conb.2006.10.007

Ermentrout, Bard.(2002). *Simulating, analyzing, and animating dynamical systems: a guide to XPPAUT for researchers and students*. Philadelphia: Society for Industrial and Applied Mathematics.

Ermentrout, Bard, & Terman, David H.(2010). *Mathematical foundations of neuroscience*. New York: Springer.

Friesen, W. O.(1994). Reciprocal inhibition: a mechanism underlying oscillatory animal movements. *Neurosci Biobehav Rev, 18*(4), 547–553.

Grillner, S., Markram, H., De Schutter, E., Silberberg, G., & LeBeau, F. E.(2005). Microcircuits in action–from CPGs to neocortex. *Trends Neurosci, 28*(10), 525–533. doi: S0166–2236(05)00211–0 [pii] 10.1016/j.tins.2005.08.003

Guckenheimer, John, & Holmes, Philip.(1997). *Nonlinear oscillations, dynamical systems, and bifurcations of vector fields*(Corr. 5th print. ed.). New York: Springer.

Kintos, N., Nusbaum, M. P., & Nadim, F.(2008). A modeling comparison of projection neuron- and neuromodulator-elicited oscillations in a central pattern generating network. *J Comput Neurosci, 24*(3), 374–397. doi: 10.1007/s10827–007–0061–7

Mamiya, A., & Nadim, F.(2004). Dynamic interaction of oscillatory neurons coupled with reciprocally inhibitory synapses acts to stabilize the rhythm period. *J Neurosci, 24*(22), 5140–5150.

Manor, Y., Nadim, F., Epstein, S., Ritt, J., Marder, E., & Kopell, N. (1999). Network oscillations generated by balancing graded asymmetric reciprocal inhibition in passive neurons. *J Neurosci, 19*(7), 2765–2779.

Marder, E., & Calabrese, R. L.(1996). Principles of rhythmic motor pattern generation. *Physiol Rev, 76*(3), 687–717.

Mishchenko, E., & Rozov, N.(1997). *Differential Equations with Small Parameters and Relaxation Oscillations*. New York: Plenum Press.

Oprisan, S. A., Thirumalai, V., & Canavier, C. C.(2003). Dynamics from a time series: can we extract the phase resetting curve from a time series? *Biophys J, 84*(5), 2919–2928. doi: S0006–3495(03)70019–8 [pii] 10.1016/S0006–3495(03)70019–8

Pinsker, H. M.(1977). Aplysia bursting neurons as endogenous oscillators. I. Phase-response curves for pulsed inhibitory synaptic input. *J Neurophysiol, 40*(3), 527–543.

Prinz, A. A., Thirumalai, V., & Marder, E.(2003). The functional consequences of changes in the strength and duration of synaptic inputs to oscillatory neurons. *J Neurosci, 23*(3), 943–954.

Somers, D., & Kopell, N.(1993). Rapid synchronization through fast threshold modulation. *Biol Cybern, 68*(5), 393–407.

Thirumalai, V., Prinz, A. A., Johnson, C. D., & Marder, E.(2006). Red pigment concentrating hormone strongly enhances the strength of the feedback to the pyloric rhythm oscillator but has little effect on pyloric rhythm period. *J Neurophysiol, 95*(3), 1762–1770.

Wang, X. J., & Buzsaki, G.(1996). Gamma oscillation by synaptic inhibition in a hippocampal interneuronal network model. *J Neurosci, 16*(20), 6402–6413.

Whittington, M. A., Traub, R. D., Kopell, N., Ermentrout, B., & Buhl, E. H.(2000). Inhibition-based rhythms: experimental and mathematical observations on network dynamics. *Int J Psychophysiol, 38*(3), 315–336. doi: S0167876000001732 [pii]

Zhou, L., LoMauro, R. and Nadim, F.(2006). The interaction between facilitation and depression of two release mechanisms in a single synapse. *Neurocomputing, 69*, 1001–1005.